Chemical Physics Letters 512 (2011) 49–53

Contents lists available at ScienceDirect

Chemical Physics Letters

journal homepage: www.elsevier.com/locate/cplett

On the electronic structure of mono-rhenium oxide clusters: ReO_n^- and ReO_n (n = 3, 4)

Wen-Jie Chen [a,b], Hua-Jin Zhai [c], Xin Huang [a,b,*], Lai-Sheng Wang [c,*]

[a] Department of Chemistry, Fuzhou University, Fuzhou, Fujian 350108, PR China
[b] State Key Laboratory of Structural Chemistry, Fuzhou, Fujian 350002, PR China
[c] Department of Chemistry, Brown University, Providence, RI 02912, USA

ARTICLE INFO

Article history:
Received 10 March 2011
In final form 5 July 2011
Available online 13 July 2011

ABSTRACT

We report a photoelectron spectroscopy and density-functional study on mono-rhenium oxide clusters: ReO_n^- and ReO_n (n = 3, 4). Electron affinities of ReO_3 and ReO_4 are measured to be 3.53 ± 0.05 and 5.58 ± 0.03 eV. ReO_3^- is shown to possess a planar D_{3h} ($^1A_1'$) ground state and ReO_3 adopts a nonplanar C_{3v} ($^2A_1$) structure. ReO_4^- has T_d ($^1A_1$) structure, whereas ReO_4 has C_s ($^2A'$) symmetry due to Jahn–Teller effects and contains a Re–O· radical unit. Localized Re 5d electrons in ReO_3^- and ReO_3 give rise to Re^{5+} and Re^{6+} centers, making them simple models for O_2 activation.

1. Introduction

Rhenium oxides are used as industrial catalysts for olefin metatheses [1–3], and have been examined as well for other catalytic reactions such as hydrogenation, selective reduction of NO_x, and oxidation reactions. The prominent rhenium oxo-compound, methyltrioxorhenium (MTO, CH_3ReO_3), represents one of the most versatile oxidation catalysts known to date [4–6]. However, the underlying mechanisms and kinetics of many rhenium oxide catalytic processes are still not well understood. Gas-phase clusters can be used as effective models toward mechanistic understanding of catalysis at the molecular level [7]. Mono-rhenium oxide clusters have been studied in a number of previous works, both experimentally [8–12] and theoretically [9,12,13]. Collision induced dissociation (CID) and ligand exchange reactions were conducted for a series of rhenium–oxygen complex cations, $Re(O_2)^+$, $Re(O_2)_2^+$, $Re(O_2)_3^+$, $Re(O_2)_4^+$, ReO_3^+, and $ReO_3(O_2)^+$, revealing ReO_3^+ as a stable core for the ReO_5^+ complex [8]. The ReO_2^- and ReO_3^- cluster anions were studied using photoelectron spectroscopy (PES), yielding electron affinities of 2.5 ± 0.1 and 3.6 ± 0.1 eV for ReO_2 and ReO_3, respectively [11]. Matrix infrared spectra were reported for Re, Ru, and Os oxide molecules, including ReO_3^- and ReO_4^- [12].

We are interested in probing the structural and electronic properties of early transition metal oxide clusters [14–22], aiming at providing controllable molecular models for mechanistic insight into oxide catalysis [23]. In the current study, we combine anion PES with density-functional theory (DFT) calculations to elucidate the structures and bonding in the simplest rhenium oxide clusters: ReO_n^- and ReO_n (n = 3, 4). The electron affinity of ReO_4 is measured to be very high (5.58 ± 0.03 eV), suggesting that this neutral cluster is an extremely strong oxidizer and belongs to the class of high electron affinity species called superhalogen [24,25]. DFT calculations show that ReO_3^- and ReO_4^- possess D_{3h} and T_d symmetries, respectively, with classical oxo Re=O bonds. The ReO_4 cluster features an elongated Re–O· oxyl bond with oxygen radical character. The ReO_3^- and ReO_3 clusters possess two and one localized Re 5d electrons, respectively, and provide well-defined Re^{5+} and Re^{6+} centers. The localized 5d electrons can be transferred to an approaching O_2 molecule, making ReO_3^- and ReO_3 simple cluster models for O_2 activation.

2. Experimental and computational methods

2.1. Photoelectron spectroscopy

The experiment was carried out using a magnetic-bottle-type PES apparatus equipped with a laser vaporization cluster source, details of which were described elsewhere [26]. Briefly, $Re_mO_n^-$ type anion clusters were produced by laser vaporization of a rhenium disk target in the presence of a helium carrier gas seeded with 0.5% O_2. The cluster anions were analyzed using a time-of-flight mass spectrometer. The ReO_3^- and ReO_4^- clusters of current interest were each mass-selected and decelerated before being photodetached. The photodetachment experiment was conducted at 193 nm (6.424 eV) from an ArF excimer laser. Effort was made to choose colder clusters (that is, those with long resident times in the nozzle) for photodetachment, which was shown previously to be critical for obtaining high quality PES data. Photoelectrons were collected at nearly 100% efficiency by the magnetic-bottle

* Corresponding authors. Address: Department of Chemistry, Brown University, Providence, RI 02912, USA (L.-S. Wang).
E-mail addresses: xhuang@fzu.edu.cn (X. Huang), lai-sheng_wang@brown.edu (L.-S. Wang).

0009-2614/$ - see front matter © 2011 Elsevier B.V. All rights reserved.
doi:10.1016/j.cplett.2011.07.018

and analyzed in a 3.5 m long electron flight tube. The PES spectra were calibrated using the known spectrum of Au^-, and the energy resolution of the apparatus was $\Delta E_k/E_k \sim 2.5\%$, that is, ~25 meV for 1 eV electrons.

2.2. Density functional theory calculations

Theoretical calculations were performed at the DFT level using the hybrid B3LYP functional [27–29]. A number of structural candidates including different spin states and initial structures were evaluated, and the search for the global minima was performed using analytical gradients with the Stuttgart relativistic small core potential and the valence basis sets [30,31] augmented with two *f*-type and one *g*-type polarization functions [$\zeta(f) = 0.327$, 0.955; $\zeta(g) = 0.636$] for Re as recommended by Martin and Sundermann [32] and the aug-cc-pVTZ basis set for oxygen [33,34]. Scalar relativistic effects, that is, the mass velocity and Darwin effects, were taken into account via the quasi-relativistic pseudo-potentials. Vibrational frequency calculations were performed at the same level of theory to verify the nature of the stationary points. Vertical detachment energies (VDEs) were calculated using the generalized Koopmans' theorem by adding a correction term to the eigenvalues of the anion [35]. The correction term was estimated by $\delta E = E_1 - E_2 - \varepsilon_{HOMO}$, where E_1 and E_2 are the total energies of the anion and neutral, respectively, in their ground states at the anion equilibrium geometry and ε_{HOMO} corresponds to the eigenvalue of the highest occupied molecular orbital (HOMO) of the anion. To assure the reliability of the calculated VDEs, we performed additional calculations using the smaller basis sets, that is, the effective core potential (ECP) basis set Lanl2dz for Re and 6-31G for O. It is stressed that all calculated eigenvalues of the occupied orbitals are negative, for both the large Re/Stuttgart + 2*f*1g/O/aug-cc-pVTZ and the smaller Re/Lanl2dz/O/6-31G basis sets, and the eigenvalues appear to be relatively insensitive to the choice of basis sets. This is in contrast to the cases of atomic anions, for which the applicability of DFT has been controversial [36,37]. Only the B3LYP/Re/Stuttgart + 2*f*1g/O/aug-cc-pVTZ results will be presented in this Letter. All calculations were performed with the GAUSSIAN 03 software package [38]. Three-dimensional contours of the molecular orbitals (MOs) were visualized using the VMD software [39].

3. Experimental results

The PES spectra of the ReO_3^- and ReO_4^- clusters at 193 nm are shown in Figure 1. The observed spectral bands are labeled with letters, X and A. The measured adiabatic detachment energies (ADEs) and VDEs are summarized in Table 1, where they are compared with theoretical data at the B3LYP level.

The PES spectrum of ReO_3^- (Figure 1a) exhibits two well separated bands: X and A. Both bands are reasonably sharp, and band X shows substantially higher intensity relative to band A. The VDEs for bands X and A are measured from their well-defined band maxima to be 3.62 and 6.08 eV, respectively (Table 1). Since no vibrational structures are resolved for band X, the ground-state ADE is evaluated by drawing a straight line along its leading edge and then adding the instrumental resolution to the intersection with the binding energy axis. The ADE thus evaluated is 3.53 ± 0.05 eV, which represents the electron affinity of the ReO_3 neutral cluster. Similarly, the ADE for band A is evaluated to be 6.01 ± 0.02 eV. The ADE difference between bands X and A defines a large excitation energy of 2.48 eV.

The electron binding energy for ReO_4^- turns out to be extremely high, as shown in Figure 1b. Only one band (X) is observed, which appears much broader than those of ReO_3^- (Figure 1a). The ground-state VDE is measured from the band maximum to be 5.83 eV

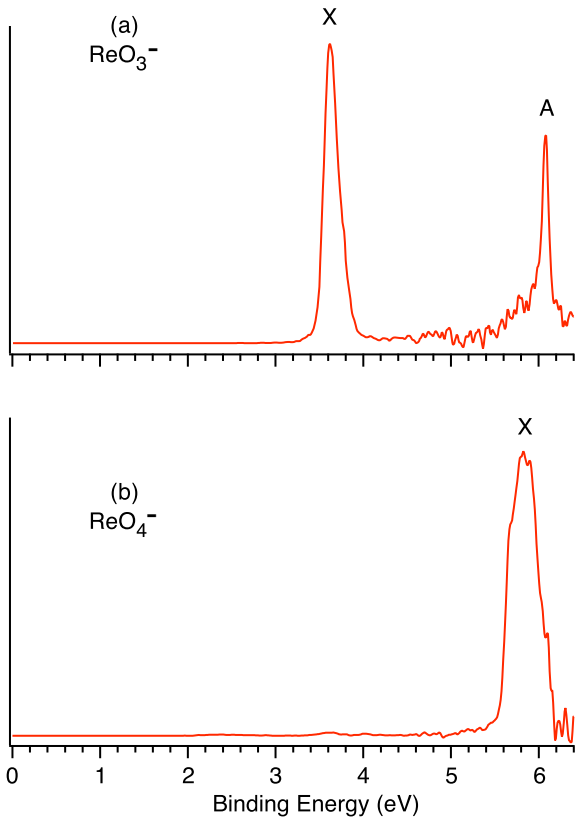

Figure 1. Photoelectron spectra of (a) ReO_3^- and (b) ReO_4^- at the 193 nm (6.424 eV).

Table 1
Experimental adiabatic and vertical detachment energies (ADEs and VDEs) from the photoelectron spectra of ReO_3^- and ReO_4^-, and comparison with the theoretical values at the B3LYP level.

	Exptl[a,b]			Theor[a,c]		
	Feature	ADE	VDE	ADE	MO	VDE
ReO_3^-	X	3.53 (5)[d]	3.62 (5)	3.50[d]	$5a_1'$	3.63
(D_{3h}, $^1A_1'$)	A	6.01 (2)[e]	6.08 (2)		$1a_2'$	5.83
					$5e'$	6.02
					$2a_2''$	6.20
ReO_4^-	X	5.58 (3)[d]	5.83 (3)	5.65[d]	$1t_1$	5.83
(T_d, $^1A_1$)					$5t_2$	6.48

[a] All energies are in eV.
[b] Numbers in the parentheses represent experimental uncertainties in the last digit.
[c] The ground-state electron configurations for the anions are $\ldots(2a_2'')^2(5e')^4(1a_2')^2(5a_1')^2$ for ReO_3^- and $\ldots(5t_2)^6(1t_1)^6$ for ReO_4^-.
[d] Electron affinity of the neutral cluster.
[e] The X–A energy gap of ReO_3 is defined by the ADE difference to be 2.48 ± 0.05 eV.

(Table 1). The ground-state ADE is evaluated from the well-defined band onset as 5.58 ± 0.03 eV, which is the electron affinity of the ReO_4 neutral cluster.

4. Theoretical results

4.1. ReO_3^- and ReO_3

The ground state of ReO_3^- is predicted to be a planar D_{3h} ($^1A_1'$) closed-shell structure (Figure 2a), consistent with that from previous DFT calculations by Zhou et al. [12]. The Re–O bond length is 1.733 Å. The lowest triplet state of ReO_3^- (C_s, $^3A'$) is 1.67 eV higher

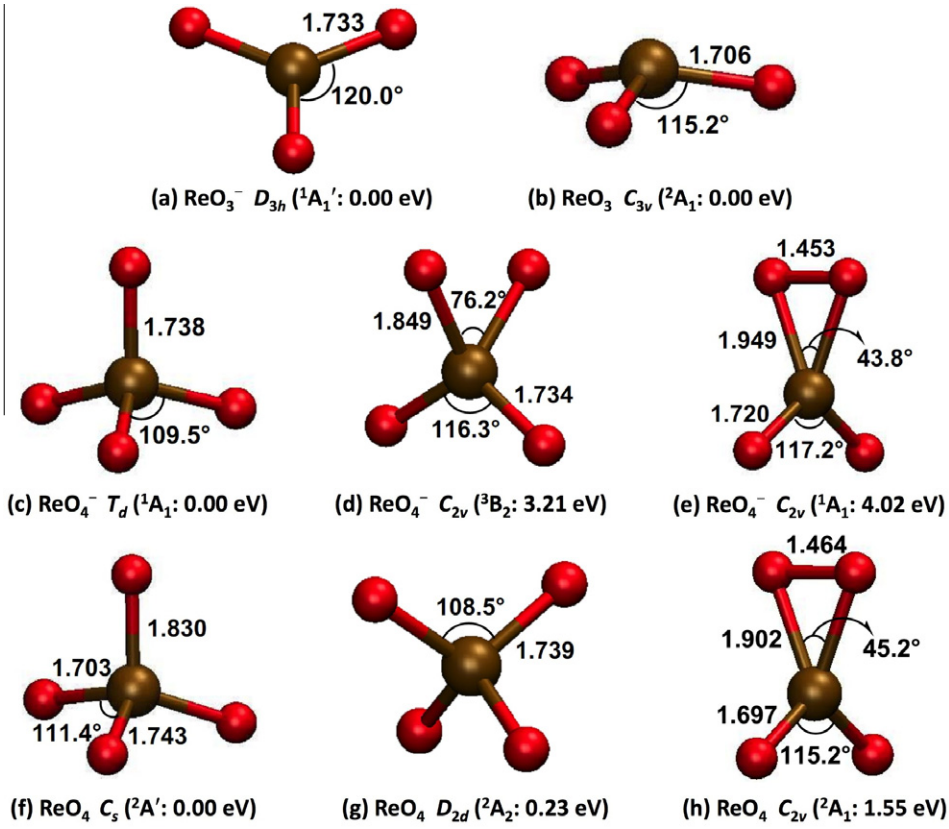

Figure 2. Optimized global minima and selected higher energy structures for ReO_n^- and ReO_n (n = 3, 4) at the B3LYP level of theory. Bond lengths (Å) and bond angles (°) are shown.

in energy (not shown). The neutral ReO_3 cluster is found to have a doublet ground state, (C_{3v}, $^2A_1$) (Figure 2b), also in agreement with the previous calculations [12]. The planar D_{3h} neutral structure is a transition state for inversion with a low out-of-plane imaginary vibrational frequency ($-143.1i$ cm^{-1}) and a small energy barrier (~0.1 eV). The Re–O bond length for neutral ReO_3 (1.706 Å) is decreased by about 0.03 Å as compared to the anion. Significant anion-to-neutral geometric change occurs in the out-of-plane angle for ReO_3, with a dihedral angle of 24.6° between the OReO and OOO planes, showing a pyramidalization at the central Re site in the neutral cluster.

4.2. ReO_4^- and ReO_4

Using the isomeric structures of ReO_3^- as the starting points, we searched the potential energy surfaces for $ReO_4^{-/0}$ and located a number of isomers. Selected structures are shown in Figure 2. The ground state of ReO_4^- is predicted to be T_d ($^1A_1$) symmetry (Figure 2c) with a Re–O bond length of 1.738 Å, consistent with the previous calculations [12]. Alternative structures for ReO_4^- are well separated in energy from the ground state (>3 eV). The lowest triplet state, C_{2v} ($^3B_2$) (Figure 2d), with the four oxygen atoms bonded to Re in a distorted tetrahedron, is 3.21 eV above the ground state. A singlet structure with a di-oxygen (O–O) bond [C_{2v} ($^1A_1$), Figure 2e] is found to be 4.02 eV higher in energy, in which the peroxo O–O bond length is calculated to be 1.453 Å, close to that of the peroxide anion (~1.49 Å).

For neutral ReO_4, the ground state is predicted to be a doublet state, C_s ($^2A'$) (Figure 2f), which is distorted from the T_d symmetry due to the Jahn–Teller effect, in agreement with a recent theoretical study [13]. The distortion leads to two kinds of Re–O bonds: one with the longer bond (1.830 Å), which we label as oxyl (–O·) oxygen, and three as oxo (=O) oxygen atoms with shorter bonds (1.703, 1.703, and 1.743 Å). A D_{2d} ($^2A_2$) structure with the Re–O bond lengths of 1.739 Å is predicted to lie 0.23 eV above the neutral ground state (Figure 2g). In addition, a doublet dioxide peroxo (O_2)ReO_2 structure (Figure 2h) is found to be 1.55 eV above the ground state.

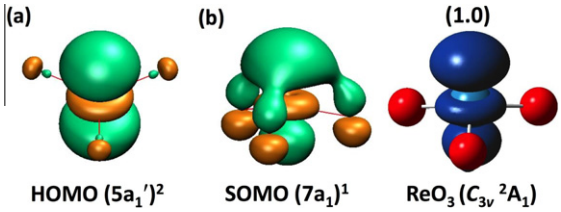

Figure 3. (a) The HOMO picture of the ReO_3^- (D_{3h}, $^1A_1'$) anion. (b) The SOMO picture and spin densities of the neutral ReO_3 (C_{3v}, $^2A_1$) cluster. The numerical spin densities are shown (in parentheses) in |e|. Blue represents the location of maximum density. (For interpretation of the references to color in this figure legend, the reader is referred to the web version of this article.)

5. Comparison between experiment and theory

While anion clusters are challenging for the standard DFT methods, for transition metal systems the DFT methods remain the default choice. Recent benchmarking studies have shown that different DFT methods (such as pure DFT versus hybrid DFT) are highly complimentary with each other, and the key is to choose an appropriate method for a particular system [40,41]. B3LYP appears to perform well for Re oxide clusters. The ground state of ReO_3^- is D_{3h} ($^1A_1'$) with a valent electron configuration

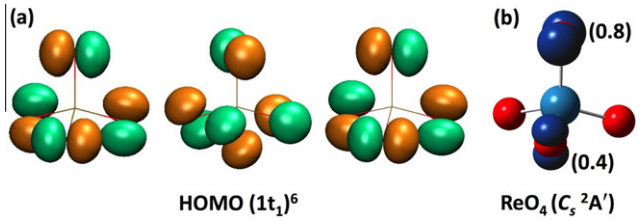

Figure 4. (a) The pictures of the degenerate HOMO orbitals of the ReO_4^- (T_d, $^1A_1$) anion. (b) Spin densities of the ReO_4 (C_s, $^2A'$) neutral cluster. The numerical spin densities over O atoms are shown (in parentheses) in |e|. Blue represents the location of maximum density. (For interpretation of the references to color in this figure legend, the reader is referred to the web version of this article.)

$\ldots(2a_2'')^2(5e')^4(1a_2')^2(5a_1')^2$, where the $5a_1'$ HOMO (Figure 3a) is nonbonding mainly composed out of the d_{z^2} atomic orbital of Re. All deeper MOs are of O 2p character. The ReO_3 neutral is predicted to be a doublet (C_{3v}, $^2A_1$) with an electron configuration $\ldots(6a_1)^2(6e)^4(1a_2)^2(7a_1)^1$. The half-occupation of the $7a_1$ MO induces a distortion in which Re is substantially out of the plane (24.6°) defined by the three oxygen atoms (Figure 2b). There are only minor changes in the Re–O bond length between ReO_3 and ReO_3^-, and thus the Franck–Condon envelope for the ground-state transition should be dominated by the inversion mode. The ADE and VDE for electron detachment from the $5a_1'$ MO are predicted as 3.50 and 3.63 eV (Table 1), respectively, in excellent agreement with the experimental data (ADE: 3.53 ± 0.05 eV; VDE: 3.62 eV). Pramann et al. [11] previously reported an electron affinity of 3.6 ± 0.1 eV for ReO_3. The first excited state of ReO_3 (band A; Figure 1a) is observed at a VDE of 6.08 eV, which should be assigned to electron detachment from the ($1a_2'$) orbital (calculated VDE: 5.83 eV). It seems that the calculation underestimates the higher VDEs by more than 0.25 eV. Assuming similar theoretical errors, we predicted that detachments from the $5e'$ and $2a_2''$ orbitals are probably not accessible in the current experiment.

The ReO_4^- anion is a stoichiometric molecule. The ground state of ReO_4^- is predicted to be closed-shell T_d ($^1A_1$) with a valent electron configuration $\ldots(5t_2)^6(1t_1)^6$, which primarily consist of O 2p characters. The triply degenerate HOMO ($1t_1$) orbitals are depicted in Figure 4a. The calculated ground-state ADE and VDE upon detachment from the $1t_1$ HOMO are 5.65 and 5.83 eV, respectively, in excellent agreement with the experimental measurements (ADE: 5.58 ± 0.03 eV; VDE: 5.83 eV). Removal of an electron from the tetrahedral T_d ReO_4^- results in a Jahn–Teller effect, distorting the neutral to a lower C_s symmetry, consistent with the relatively broad ground-state PES band (Figure 1b). The next detachment channel is from $5t_2$ with a calculated VDE of 6.48 eV, which is experimentally not accessible at the 193 nm (6.424 eV) photon energy.

6. Discussion

6.1. The PES spectrum of ReO_3^- and comparison with the electronic structure of ReO_3 bulk oxide

The PES spectrum of ReO_3^- exhibits two bands with distinct electron binding energies: X (VDE: 3.62 eV) versus A (VDE: 6.08 eV). The X band is from the metal-based d_{z^2} lone pair (Figure 3a) and the A band is from O 2p type orbitals. Our prior PES studies on metal oxide clusters have shown that metal-based PES bands are normally well separated from the O 2p-based ones, and the latter appear at much higher binding energies (typically >5 eV) [14–19]. The ADE difference between bands X and A defines the electronic excitation energy (2.48 eV; Table 1) for the ReO_3 neutral cluster, which is the molecular analog of the energy gap between the Re 5d conduction band and the O 2p valence band of bulk ReO_3 oxide.

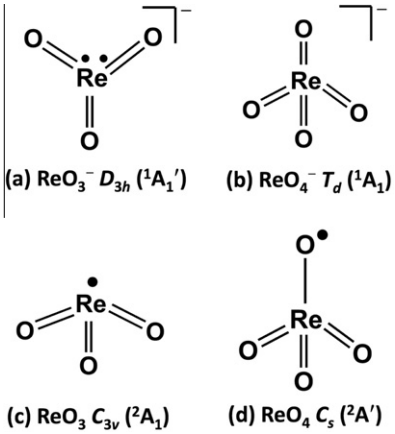

Figure 5. Valence-bond descriptions of ReO_n^- and ReO_n ($n = 3, 4$). Bond orders, unpaired electrons, and lone pair are indicated.

Rhenium trioxide crystallizes in a simple cubic lattice [42], comprising of a network of corner-sharing ReO_6 octahedra. The ReO_3 oxide is unique in that it is the only stable trioxide of the group VIIB elements (Mn, Tc, and Re) and it behaves as a metal because of the availability of one 5d electron on each Re center. Optical reflectivity measurements of the ReO_3 single crystal by Feinleib et al. [43] revealed an interband threshold of about 2 eV. Interestingly, the energy separation we observed for the gas-phase ReO_3 cluster (2.48 eV) is comparable to that of the bulk ReO_3 oxide.

6.2. On the high electron affinity of ReO_4

The perrhenate anion, ReO_4^-, dominates the chemistry of rhenium [44]. However, the exact value of the electron affinity of ReO_4 has been elusive. An early ion–molecule reactivity study in 1972 suggested a lower limit of the electron affinity of ReO_4 to be 2.5 eV [45]. This was refined later in 1975 on the basis of thermochemical data to be 4.46 ± 0.50 eV (430 ± 50 kJ/mol) [46]. The current PES measurement yields an electron affinity of 5.58 ± 0.03 eV for ReO_4, as is also borne out from our theoretical calculation, which is far greater than the previously known values (by ~1.1 eV). The electron affinity of ReO_4 is among the highest ever reported in the gas phase [47], suggesting that this neutral cluster is an extremely strong oxidizer and belongs to the class of novel chemical species called superhalogens [24,25]. It should be noted that the electron affinity of ReO_4 is substantially higher than that of its valent isoelectronic 3d counterpart MnO_4 (electron affinity: 4.80 ± 0.10 eV) [48]. The current measurement suggests that ReO_4^- is a more stable anion than MnO_4^-, which appears to be consistent with their known chemistries, that is, the ReO_4^- anion is more stable in solution than MnO_4^-.

6.3. Chemical bonding in ReO_n^- and ReO_n ($n = 3, 4$)

The Re–O bonding in bulk Re oxides involves both ionic and covalent characters. For the simple mono-rhenium oxide clusters, ReO_n^- and ReO_n ($n = 3, 4$), the chemical bonding can be understood using the valence-bond description as schematically shown in Figure 5. In ReO_3^-, the valence electrons of Re form three Re=O double bonds and an electron lone pair on the Re center (Figure 5a), resulting in a closed-shell, planar D_{3h} ($^1A_1'$) structure. Removal of an electron from the d_{z^2} orbital of Re gives rise to a significantly nonplanar configuration in the ReO_3 neutral cluster (Figure 5c), but no significant changes occur in the Re–O bond length between ReO_3 and

ReO_3^- and thus the three Re=O terminal bonds retain intact in ReO_3.

In the stoichiometric ReO_4^- anion, all the valence electrons on Re are used to form Re=O double bonds, resulting in a highly stable tetrahedral molecule (Figure 5b). Removal of an electron from ReO_4^- destabilizes the tetrahedral symmetry in the ReO_4 neutral, due to the Jahn–Teller effect. Interestingly, the ReO_4 neutral cluster features three Re=O double bonds and an elongated Re–O· bond (Figures 2 and 5d). The nature of the Re–O· bond is clearly seen from the numerical spin density on the O· radical: 0.8 |e| (Figure 4b). This situation is in contrast to its valent isoelectronic WO_4^- anion, where the unpaired electron is delocalized over two oxyl O atoms [14]. The subtle discrepancy between the ReO_4 and WO_4^- structure may be caused by the different M–O bond strengths. Indeed, the Re=O bond (627 ± 84 kJ/mol) is weaker than the W=O bond (720 ± 71 kJ/mol) [49].

As shown in Figure 3, MO analysis shows that Re 5d electrons in ReO_3^- and ReO_3 are essentially localized on the Re center, giving rise to well-defined Re^{5+} and Re^{6+} sites, respectively. These sites should be chemically active and may act as simple molecular models for catalytic centers in bulk catalysts such as the Re^{5+}-oxo complexes. The localized 5d electrons on the Re^{5+} and Re^{6+} sites may be readily transferred to the π^* orbital of an approaching O_2 molecule, which would activate O_2 and yield peroxide $(ReO_3)^+(O_2)^{2-}$ and superoxide $(ReO_3)^+(O_2)^-$ complexes, respectively.

7. Conclusions

Anion photoelectron spectroscopy has been combined with density-functional theory calculations to study the electronic structure and chemical bonding of the simplest rhenium oxide clusters: ReO_n^- and ReO_n ($n = 3, 4$). The experimentally measured adiabatic and vertical detachment energies for both anions are important physical properties of rhenium oxide species. DFT calculations predict that the ReO_3^- and ReO_3 clusters possess D_{3h} ($^1A_1'$) and C_{3v} ($^2A_1$) ground states with three oxo Re=O bonds, respectively. A tetrahedral coordination environment is found for ReO_4^- and ReO_4, which possess T_d ($^1A_1$) and C_s ($^2A'$) ground states, respectively. An oxyl Re–O· unit with oxygen radical character is revealed for ReO_4. The 5d electrons in ReO_3^- and ReO_3 clusters are shown to localize on the Re center, giving rise to simple molecular models for Re^{5+} and Re^{6+} centers.

Acknowledgments

This work was supported by the Chemical Sciences, Geosciences and Biosciences Division, Office of Basic Energy Sciences, U.S. Department of Energy under grant No. DE-FG02-03ER15481 (catalysis center program). X.H. gratefully acknowledges supports from the Natural Science Foundation of China (21071031 and 90922022) and the Natural Science Foundation of Fujian Province of China (No. 2008J0151).

References

[1] J.A. Moulijn, J.C. Mol, J. Mol. Catal. 46 (1988) 1.
[2] J.C. Mol, Catal. Today 51 (1999) 289.
[3] W.A. Herrmann, J.G. Kuchler, J.K. Felixberger, E. Herdtweck, W. Wagner, Angew. Chem. Int. Ed. 27 (1988) 394.
[4] K.P. Gable, Adv. Organomet. Chem. 41 (1997) 127.
[5] G.S. Owens, J. Arias, M.M. Abu-Omar, Catal. Today 55 (2000) 317.
[6] F.E. Kühn, A. Scherbaum, W.A. Herrmann, J. Organomet. Chem. 689 (2004) 4149.
[7] D.K. Böhme, H. Schwarz, Angew. Chem. Int. Ed. 44 (2005) 2336.
[8] M. Beyer, C. Berg, G. Albert, U. Achatz, S. Joos, G. Niedner-Schatteburg, V.E. Bondybey, J. Am. Chem. Soc. 119 (1997) 1466.
[9] M. Beyer, C. Berg, S. Joos, U. Achatz, W. Hieringer, G. Niedner-Schatteburg, V.E. Bondybey, Int. J. Mass Spectrom. 185–187 (1999) 625.
[10] M.K. Beyer, C.B. Berg, V.E. Bondybey, Phys. Chem. Chem. Phys. 3 (2001) 1840.
[11] A. Pramann, K. Rademann, Chem. Phys. Lett. 343 (2001) 99.
[12] M.F. Zhou, A. Citra, B.Y. Liang, L. Andrews, J. Phys. Chem. A 104 (2000) 3457.
[13] Y.X. Zhao, X.L. Ding, Y.P. Ma, Z.C. Wang, S.G. He, Theor. Chem. Acc. 127 (2010) 449.
[14] H.J. Zhai, B. Kiran, L.F. Cui, X. Li, D.A. Dixon, L.S. Wang, J. Am. Chem. Soc. 126 (2004) 16134.
[15] X. Huang, H.J. Zhai, T. Waters, J. Li, L.S. Wang, Angew. Chem. Int. Ed. 45 (2006) 657.
[16] H.J. Zhai, L.S. Wang, J. Am. Chem. Soc. 129 (2007) 3022.
[17] H.J. Zhai, J. Döbler, J. Sauer, L.S. Wang, J. Am. Chem. Soc. 129 (2007) 13270.
[18] H.J. Zhai, S.G. Li, D.A. Dixon, L.S. Wang, J. Am. Chem. Soc. 130 (2008) 5167.
[19] H.J. Zhai, X.H. Zhang, W.J. Chen, X. Huang, L.S. Wang, J. Am. Chem. Soc. 133 (2011) 3085.
[20] X. Huang, H.J. Zhai, B. Kiran, L.S. Wang, Angew. Chem. Int. Ed. 44 (2005) 7251.
[21] H.J. Zhai, B.B. Averkiev, D.Yu. Zubarev, L.S. Wang, A.I. Boldyrev, Angew. Chem. Int. Ed. 46 (2007) 4277.
[22] D.Yu. Zubarev, B.B. Averkiev, H.J. Zhai, L.S. Wang, A.I. Boldyrev, Phys. Chem. Chem. Phys. 10 (2008) 257.
[23] For a recent frontiers article, see: H.J. Zhai, L.S. Wang, Chem. Phys. Lett. 500 (2010) 185.
[24] G.L. Gutsev, A.I. Boldyrev, Chem. Phys. 56 (1981) 277.
[25] G.L. Gutsev, A.I. Boldyrev, Adv. Chem. Phys. 61 (1985) 169.
[26] L.S. Wang, H.S. Cheng, J. Fan, J. Chem. Phys. 102 (1995) 9480.
[27] A.D. Becke, J. Chem. Phys. 98 (1993) 1372.
[28] C. Lee, W. Yang, R.G. Parr, Phys. Rev. B 37 (1988) 785.
[29] P.J. Stephens, F.J. Devlin, C.F. Chabalowski, M.J. Frisch, J. Phys. Chem. 98 (1994) 11623.
[30] D. Andrae, U. Haeussermann, M. Dolg, H. Stoll, H. Preuss, Theor. Chim. Acta 77 (1990) 123.
[31] W. Küchle, M. Dolg, H. Stoll, H. Preuss, Pseudopotentials of the Stuttgart/Dresden Group 1998, revision August 11, 1998. <http://www.theochem.uni-stuttgart.de/pseudopotential>.
[32] J.M.L. Martin, A. Sundermann, J. Chem. Phys. 114 (2001) 3408.
[33] T.H. Dunning Jr., J. Chem. Phys. 90 (1989) 1007.
[34] R.A. Kendall, T.H. Dunning Jr., R.J. Harrison, J. Chem. Phys. 96 (1992) 6796.
[35] D.J. Tozer, N.C. Handy, J. Chem. Phys. 109 (1998) 10180.
[36] J.M. Galbraith, H.F. Schaefer III, J. Chem. Phys. 105 (1996) 862.
[37] N. Rösch, S.B. Trickey, J. Chem. Phys. 106 (1997) 8940.
[38] M.J. Frisch et al., GAUSSIAN 03, Revision D.01, GAUSSIAN, Inc., Wallingford, CT, 2004.
[39] VMD (Visual Molecular Dynamics), W. Humphrey, A. Dalke, K. Schulten, J. Mol. Graphics 14 (1996) 33.
[40] S.G. Li, D.A. Dixon, J. Phys. Chem. A 111 (2007) 11908.
[41] S.G. Li, H.J. Zhai, L.S. Wang, D.A. Dixon, J. Phys. Chem. A 113 (2009) 11273.
[42] J.E. Jørgensen, J.D. Jorgensen, B. Batlogg, J.P. Remeika, J.D. Axe, Phys. Rev. B 33 (1986) 4793.
[43] J. Feinleib, W.J. Scouler, A. Ferretti, Phys. Rev. 165 (1968) 765.
[44] G. Rouschias, Chem. Rev. 74 (1974) 531.
[45] R.E. Center, J. Chem. Phys. 56 (1972) 371.
[46] R.K. Gould, W.J. Miller, J. Chem. Phys. 62 (1975) 644.
[47] J.C. Rienstra-Kiracofe, G.S. Tschumper, H.F. Schaefer III, S. Nandi, G.B. Ellison, Chem. Rev. 102 (2002) 231.
[48] G.L. Gutsev, B.K. Rao, P. Jena, X.B. Wang, L.S. Wang, Chem. Phys. Lett. 312 (1999) 598.
[49] Y.R. Luo, in: W.M. Haynes (Ed.), CRC Handbook of Chemistry and Physics, 91st Edn., CRC Press, Boca Raton, FL, 2010.